

Spectral spacing correlations for chaotic and disordered systems

O. Bohigas^a, P. Leboeuf^a and M. J. Sánchez^b

^a*Laboratoire de Physique Théorique et Modèles Statistiques¹, Bât. 100,
Université de Paris-Sud, 91405 Orsay Cedex, France*

^b*Departamento de Física J. J. Giambiagi, Facultad de Ciencias Exactas y Naturales,
Universidad de Buenos Aires, Ciudad Universitaria, 1428 Buenos Aires, Argentina.*

Abstract

New aspects of spectral fluctuations of (quantum) chaotic and diffusive systems are considered, namely autocorrelations of the spacing between consecutive levels or spacing autocovariances. They can be viewed as a discretized two point correlation function. Their behavior results from two different contributions. One corresponds to (universal) random matrix eigenvalue fluctuations, the other to diffusive or chaotic characteristics of the corresponding classical motion. A closed formula expressing spacing autocovariances in terms of classical dynamical zeta functions, including the Perron-Frobenius operator, is derived. It leads to a simple interpretation in terms of classical resonances. The theory is applied to zeros of the Riemann zeta function. A striking correspondence between the associated classical dynamical zeta functions and the Riemann zeta itself is found. This induces a resurgence phenomenon where the lowest Riemann zeros appear replicated an infinite number of times as resonances and sub-resonances in the spacing autocovariances. The theoretical results are confirmed by existing “data”. The present work further extends the already well known semiclassical interpretation of properties of Riemann zeros.

To appear in the Gutzwiller Festschrift, a special Issue of Foundations of Physics.

¹Unité de recherche de l'Université de Paris XI associée au CNRS

I. INTRODUCTION

Spectral fluctuations of classically chaotic or diffusive quantum systems have been extensively studied in the past. One of the main outcomes of these investigations has been to establish energy (or time) scales for which universal properties hold and which are reproduced by random matrix theories (RMT), to be distinguished from those which are system dependent and in many cases can be treated by semiclassical theories à la Gutzwiller⁽¹⁾. Apart from the one-point function or level density ρ which gives the global behavior and sets the main scale (its average $\bar{\rho}$ defines the mean spacing $\bar{D} = \bar{\rho}^{-1}$, or its conjugate variable defines the Heisenberg time $T_H = h\bar{\rho}$, with h the Planck constant), much emphasis has been put on the two-point function $R_2(\epsilon)$ or density-density correlation function or on quantities therefrom derived ($R_2(\epsilon)d\epsilon$ is proportional to the probability of finding two levels separated by a distance in the interval $[\epsilon, \epsilon + d\epsilon]$). One important exception to this is constituted by the nearest neighbor spacing distribution $p(s)$ ($p(s)$ is not a two-point function). It has been thoroughly investigated and its exact short and long range behavior have simple analytical forms for the Gaussian Ensembles. The short range behavior of $R_2(\epsilon)$ at the scale of one mean level spacing is the same as the one of $p(s)$, whereas the information contained in the medium and long range part of $R_2(\epsilon)$ (medium and long range correlations) is not contained in $p(s)$. It is rather well established that semiclassical theories are particularly adapted to describe medium and long range correlations whereas their ability in dealing with short range properties is dubious.

Studies of autocovariances $C(n)$ of the spacing between consecutive levels, namely quantities related to the average value of $s_m s_{m+n}$, where $s_m = t_m - t_{m-1}$, are scarce (t_m denotes an eigenvalue, with $\dots \leq t_m \leq t_{m+1} \leq \dots$). As will become clear in section II.A, spacing autocovariances $C(n)$ can be viewed as a discrete version of the (continuous) two-point correlation function (cf Eq.(2.6)). This is related to the fact that the basic building block is a discrete object, a spacing between consecutive levels. The discretization on a scale of the mean level spacing induces a “smoothing” procedure, and the structures existing up to that scale are strongly suppressed. As a consequence the spacing autocovariances are particularly suited to be described by semiclassical approaches, which are usually very difficult to control on the mean spacing scale. In terms of the conjugate variable (time), the discretization amounts to introduce a cut-off at the Heisenberg time T_H .

In contrast to $R_2(\epsilon)$, exact analytical random matrix expressions for the spacing autocovariances $C(n)$, whose study is one of the main purposes of the present paper, are not known (this explains why they are usually not extracted from data). In order to proceed use will be made of a simple relation connecting spacing variances of distant eigenvalues to the number variance (Eq.(2.5)). As discussed in Ref.(2), this very general relation applies to eigenvalues of Gaussian Ensembles and also to spectra of chaotic systems, even beyond the universal regime, as well as to spectra of integrable systems (but does not hold for Poissonian spectra). It is therefore associated to the concept of spectral rigidity, characteristic of Gaussian Ensembles of random matrices and of the non-universal regime of quantized Hamiltonian systems.

This paper, which may be considered as a continuation of Ref.(2), is organized as follows. The next section starts with the general setting, definitions and relations which will be subsequently used (section II.A). In particular, we establish an approximate (but accu-

rate) relation between spacing autocovariances and the counting function variance (number variance). When applied to eigenvalues of random matrices the resulting expressions are consistent with an ansatz introduced in Ref.(2), though the precise value of constants differ because of slight differences in both treatments. Quantum systems governed by classically diffusive motion (section II.B) and by chaotic dynamics (section II.C) are subsequently studied. In the latter case the main tool used is a semiclassical approach. Because the quantities computed are less sensitive to small energy scales, we find that the simplest form of the theory, i.e. the “diagonal approximation”, provides a very accurate global description of $C(n)$. The main result of section II.C is an expression of the autocovariances in terms of two different classical dynamical zeta functions, one of them directly related to the spectrum of the Perron-Frobenius operator. The structure of $C(n)$ can thus be interpreted as a superposition of contributions of classical singular points (or resonances). Section III has initially been conceived as an illustration of what precedes. One studies properties related to the zeros of the Riemann ζ -function by interpreting them as eigenenergies of an hypothetical quantized classically chaotic system, as suggested by Berry exploiting a beautiful analogy with the Gutzwiller trace formula⁽³⁾. Expressions for the spacing autocovariances are worked out and compared to “data” provided by the extensive computations of Odlyzko⁽⁴⁾. Features encoded in spacing autocorrelations are exhibited. Most of them are new and some unsuspected. That is why we think that the content of the section has interest in its own and goes beyond its initial illustrative purpose.

II. SPACING AUTOCOVARIANCE

A. General Considerations

Consider an ordered sequence of energy levels t_i , $i = 1, 2, \dots$, having an average density of states $\bar{\rho}(t)$. We call them “energies”, but the set can be an arbitrary sequence of points on the real line not necessarily related to a quantum mechanical spectrum. From this sequence a new stationary one, having mean level spacing equal to one, is constructed by the unfolding or rectifying procedure^{(5),(6)} $x_i = \int^{t_i} \bar{\rho}(t) dt$. The sequence x_i is located around energy t in a window of size Δt , with $\Delta t \ll t$.

Our purpose is to study properties related to distances between two consecutive eigenvalues, denoted $s_m = x_m - x_{m-1}$. More precisely, we study the autocovariances $C(n)$ of two spacings between consecutive eigenvalues located n levels apart

$$C(n) = \langle (s_m - \langle s_m \rangle)(s_{m+n} - \langle s_{m+n} \rangle) \rangle = \langle s_m s_{m+n} \rangle - 1 = I(n) - 1 , \quad (2.1)$$

where $I(n)$ are the spacing autocorrelations. The brackets denote an average over different locations m of the reference spacing or, more generally, an energy average over the spectrum. Eq.(2.1) is the simplest quantity containing information on how the different spacings are correlated that can be considered (correlations among spacings of non-consecutive levels can be expressed in terms of $C(n)$ and do not contain new information). For uncorrelated spacings $C(n) = \langle s_m \rangle \langle s_{m+n} \rangle - 1 = 0$.

Consider the length S of an interval made of n consecutive spacings, $S = \sum_{i=1}^n s_i$. The variance of S can be written as

$$\sigma^2(n) = \langle S^2 \rangle - \langle S \rangle^2 = n (\langle s^2 \rangle - n) + 2 \sum_{j=1}^{n-1} (n-j) I(j), \quad n \geq 2, \quad (2.2)$$

and $\sigma^2(1) = \langle s^2 \rangle - 1$. Inversely, Eq.(2.2) allows to express the autocovariances in terms of the variance of S ,

$$C(n) = \frac{1}{2} [\sigma^2(n+1) - 2\sigma^2(n) + \sigma^2(n-1)], \quad n \geq 2, \quad (2.3)$$

$$C(1) = \frac{1}{2} [\sigma^2(2) - 2\sigma^2(1)] . \quad (2.4)$$

For eigenvalues of Gaussian Ensembles of random matrices neither $\sigma^2(n)$ nor $C(n)$ are known in closed form. Our aim is to show that an approximate (but accurate) expression for the autocovariances of spacings may be found exploiting some properties of $\sigma^2(n)$ and Eq.(2.3).

For that purpose we consider the number variance $\Sigma^2(L)$ closely related to $\sigma^2(n)$. It is defined as the variance of the random variable which counts the number of levels contained in an interval of length L located randomly in the sequence. For eigenvalues of Gaussian Ensembles of random matrices, $\Sigma^2(L)$ evaluated at integer values of its argument is related to the variance of the interval length through⁽⁷⁾

$$\Sigma^2(L = n) - \sigma^2(n) \approx 1/6 . \quad (2.5)$$

This relation is valid, in principle, for large n . However, numerical calculations as well as analytical estimates⁽²⁾ indicate that Eq.(2.5) holds also for small values of n with an error $\sim 0.01/n^2$. Eq.(2.5) was used in Ref.(2) to determine the coefficients of an ansatz for $C(n)$ in terms of a sum of inverse even powers of n . In this section we follow an alternative path. We make no ansatz, but use Eq.(2.5) to derive similar random matrix theory (RMT) expressions for the autocovariances $C(n)$. The next sections will be devoted to the incorporation of the semiclassical and diffusive contributions to the autocovariances.

Assuming that Eq. (2.5) holds, Eqs. (2.3)-(2.4) can be written

$$C(n) \approx \frac{1}{2} [\Sigma^2(n+1) - 2\Sigma^2(n) + \Sigma^2(n-1)] \quad n \geq 2, \quad (2.6)$$

$$C(1) \approx \frac{1}{2} \left[\Sigma^2(2) - 2\Sigma^2(1) + \frac{1}{6} \right] . \quad (2.7)$$

Due to the structure of Eq.(2.3) the exact value of the constant in the r.h.s. of Eq.(2.5) is immaterial for $n \geq 2$. Notice that Eqs.(2.5) and (2.6) connect quantities related to the exact location of energy levels, like $\sigma^2(n)$ or $C(n)$, to quantities which are not, like Σ^2 , and for which explicit results exist for chaotic and diffusive systems^{(8),(9)}.

Using the approximation (2.6) the autocovariances $C(n)$ are expressed in terms of the (discrete) curvature of Σ^2 evaluated at integers n . An analogous expression (up to a sign) relates for $L > 0$ the two-level cluster function⁽¹⁰⁾ $Y_2(L)$ to the (continuous) curvature of $\Sigma^2(L)$,

$$Y_2(L) = -\frac{1}{2} \frac{\partial^2 \Sigma^2}{\partial L^2} . \quad (2.8)$$

One therefore expects the properties of $C(n)$ to be closely related to the ones of Y_2 . One aim of the present paper is to identify some of their differences.

Let us recall that the Fourier transform of Y_2 defines the form factor $K(\tau)$,

$$Y_2(L) = 2 \int_0^\infty d\tau (1 - K(\tau)) \cos(2\pi L\tau) , \quad (2.9)$$

in terms of which the number variance reads

$$\Sigma^2(L) = \frac{2}{\pi^2} \int_0^\infty d\tau K(\tau) \frac{\sin^2(\pi L\tau)}{\tau^2} . \quad (2.10)$$

τ is a rescaled time in units of the Heisenberg time, $\tau = T/h\bar{\rho}$ and, correspondingly, energies are being measured in units of mean spacing $\bar{\rho}^{-1}$.

As is well known, the form factor $K(\tau)$ plays an important role in the theory of quantum dynamical systems. For disordered and chaotic systems, it contains basic information related to short time specificities. In the opposite limit, namely the ergodic (long time) regime, its behavior is universal and coincides with RMT. Accordingly, in order to exhibit the different relevant time scales, it is convenient to write

$$\Sigma^2 = \Sigma_{\text{rm}}^2 + \Sigma_{\text{nu}}^2 . \quad (2.11)$$

Σ_{rm}^2 is the random matrix result for the number variance (cf Eq.(2.15) below). The non-universal contribution Σ_{nu}^2 will be considered later on for disordered as well as for chaotic systems. From Eq.(2.6), and in analogy with Eq.(2.11) we write

$$C = C_{\text{rm}} + C_{\text{nu}} . \quad (2.12)$$

Using the exact form of Σ_{rm}^2 it is possible to obtain, through Eq.(2.6), a general expression for C_{rm} . However, we rather prefer to use an asymptotic expansion of the number variance for large values of n . In particular, this makes easier the comparison of the present approach with the results of Ref.(2). For large values of L , the leading order behavior of Σ_{rm}^2 is⁽¹⁰⁾

$$\Sigma^2(L) = \frac{2}{\beta\pi^2} \log L + \mathcal{O}(1) , \quad (2.13)$$

where $\beta = 1, 2$ and 4 denote the three types of Gaussian Ensembles, orthogonal, unitary and symplectic, respectively. Eq.(2.13), together with Eq.(2.6) leads to

$$C_{\text{rm}}^0(n) = \frac{1}{\beta\pi^2} \log \left(1 - \frac{1}{n^2} \right) , \quad (2.14)$$

valid for $n \geq 2$. For a more accurate evaluation of $C(n)$ we include more terms in the asymptotic expansion of the number variance. For example, for $\beta = 2$ we use

$$\Sigma^2(L) = \frac{1}{\pi^2} \left[\log(2\pi L) + \gamma + 1 - \frac{\cos(2\pi L)}{(2\pi L)^2} - \frac{4 \sin(2\pi L)}{(2\pi L)^3} + \mathcal{O}(1/L^4) \right] . \quad (2.15)$$

An analogous expansion can be used for $\beta = 1$. Substituting these expansions in (2.6) one gets, for $\beta = 1$ and 2

$$C_{\text{rm}}(n) = C_{\text{rm}}^0(n) + \frac{1}{\beta\pi^2} \left(\frac{\lambda_\beta}{n^4} + \frac{\alpha_\beta}{n^6} \right) + \mathcal{O}(1/n^8), \quad (2.16)$$

with λ_β and α_β given by

$$\lambda_1 = \frac{3}{2\pi^2}, \quad \alpha_1 = \frac{15}{6\pi^2} - \frac{105}{6\pi^4} \quad (2.17)$$

$$\lambda_2 = -\frac{3}{2\pi^2}, \quad \alpha_2 = -\frac{15}{6\pi^2} + \frac{135}{6\pi^4}. \quad (2.18)$$

For $\beta = 4$ a theorem relating the statistical properties of the Gaussian Ensemble with $\beta = 1$ to those of $\beta = 4$ can be exploited⁽¹¹⁾. It implies that the autocovariances are related as follows (the notation is obvious),

$$C_{\text{rm},4}(n) = \frac{1}{2} C_{\text{rm},1}(2n) + \frac{1}{4} C_{\text{rm},1}(2n-1) + \frac{1}{4} C_{\text{rm},1}(2n+1). \quad (2.19)$$

Eq.(2.19) enables to determine the coefficients in (2.16) for $\beta = 4$

$$\lambda_4 = \lambda_1/4, \quad \alpha_4 = (\alpha_1 + 5\lambda_1)/16.$$

Aside from the logarithmic leading order term, Eq.(2.15) contains sub-dominant oscillatory corrections. The latter modify the simple estimate Eq.(2.14) by adding smooth correction terms of order $\mathcal{O}(1/n^4)$ and higher according to Eq.(2.16). Contrary to this, when computing the cluster function from Eq.(2.8) these sub-dominant terms of $\Sigma^2(L)$ give rise to an oscillatory behavior of Y_2 on the scale of the mean level spacing. For example, for $\beta = 2$ we have

$$Y_2(L) = \frac{1}{2\pi^2 L^2} - \frac{\cos(2\pi L)}{2\pi^2 L^2}. \quad (2.20)$$

In contrast, there are no oscillations in $C(n)$ because Σ^2 is evaluated at integer values of its argument, and the oscillatory functions in Eq.(2.15) are either zero or one. Similar results are also found for the other symmetry classes. This makes an important difference between the RMT behavior of Y_2 and that of $C(n)$, with a suppression of the structures of Y_2 on the scale of the mean level spacing or below.

Expanding the logarithm in $C_{\text{rm}}^0(n)$ one obtains from Eq.(2.16) a series in inverse even powers of n , which is consistent with the ansatz of Ref.(2). However the coefficients in this expansion slightly differ from those obtained in Ref.(2). This difference is due to the fact that terms of $\mathcal{O}(1/n^2)$ have been ignored in Eq.(2.5). Despite its asymptotic character, Eq.(2.16) reproduces with good precision the autocovariances of spacings of random matrices down to values $n \approx 2$.

Let us finally mention that the sum-rule

$$\sum_{j=1}^{\infty} C(j) + \frac{\sigma^2(1)}{2} = 0 \quad (2.21)$$

valid for Gaussian Ensembles⁽¹²⁾, is violated in the present approach due to inaccuracies of the low ($j = 1$ and 2) terms ($C(1)$ has to be computed from Eq.(2.7)). This is in contrast with what is done in Ref.(2) where, by construction, Eq.(2.21) is fulfilled. Notice however that the procedure adopted here is much better adapted for a semiclassical description and that this apparent deficiency is of no consequence for what follows.

B. Diffusive systems

We now consider the motion of a particle confined to a spatial region of typical size R whose classical dynamics is diffusive. The classical motion is characterized by the diffusion constant D . The elastic mean free time between elastic collisions is denoted $\tau_e = T_e/T_H$ (we again measure the time in units of Heisenberg time $T_H = h\bar{\rho}$). Quantum mechanically the relevant diffusive time scale is the Thouless time, i.e. the typical time it takes to the system to cross the sample, $\tau_c = R^2/(Dh\bar{\rho})$ ($1/\tau_c = g$ is the dimensionless conductance). For a diffusive system $\tau_e \ll \tau_c \ll 1$.

Ignoring the specificities of the dynamics for extremely short times $\tau \lesssim \tau_e$ ⁽¹³⁾, for diffusive systems the form factor has, as in the chaotic case, two distinct regimes. For times $\tau \ll \tau_c$ the dynamics is diffusive (non-universal) and the form factor is given by⁽¹⁴⁾

$$K_{\text{nu}}(\tau) = \frac{2}{\beta} \left(\frac{\tau_c}{4\pi} \right)^{d/2} \tau^{1-d/2}, \quad (2.22)$$

with d the space dimension. On the other hand, for $\tau \gg \tau_c$ the ergodic regime is reached and we recover a universal behavior for $K(\tau)$ described by RMT⁽¹⁵⁾. We do not intend to describe in detail the transition between these two regimes, and simply assume $K(\tau) = K_{\text{rm}}(\tau) + K_{\text{nu}}(\tau)$ (consistently with Eq.(2.11)).

Inserting $K_{\text{rm}}(\tau)$ in (2.10) we again get Σ_{rm}^2 as in the previous subsection. On the other hand, from the diffusive form factor (2.22) we obtain Σ_{nu}^2 ,

$$\Sigma_{\text{nu}}^2(L) = \frac{4}{\beta\pi^2} \left(\frac{L\tau_c}{4\pi} \right)^{d/2} \int_0^\infty d\tau \frac{\sin^2(\pi\tau)}{\tau^{1+d/2}}. \quad (2.23)$$

The integral gives a constant $a_d = \pi, \pi^2/2$ and $4\pi^2/3$ for $d = 1, 2$ and 3 , respectively. Eq.(2.23) provides the well known⁽¹⁴⁾ asymptotic expression of the number variance for diffusive systems, $\Sigma^2 \propto (L\tau_c)^{d/2}$.

Computing the discrete curvature (2.6) we have

$$C = C_{\text{rm}} + C_{\text{dif}}. \quad (2.24)$$

C_{rm} is the random matrix autocovariance given by (2.16). C_{dif} is computed from (2.23),

$$C_{\text{dif}}(n) = \frac{a_d d(d/2 - 1)}{\beta\pi^2} \left(\frac{\tau_c}{4\pi} \right)^{d/2} \frac{1}{n^{2-d/2}}. \quad (2.25)$$

Notice that for $d = 2$ the contribution vanishes, and that it is positive for $d = 3$ and negative for $d = 1$. Though this is a decreasing function of n , its relative importance with respect to C_{rm} increases since for large separations it vanishes as $n^{-(2-d/2)}$, which is slower than the n^{-2} decay of C_{rm} . It therefore dominates the tail of the autocovariance function in any dimension (except $d = 2$). It represents a finite conductance correction to the RMT behavior, since as mentioned before $g = \tau_c^{-1}$. For $d = 3$, $C(n)$ is negative for small n (spacings separated by small distances are anti-correlated) but tends to zero from above for large distances (positive correlations between large distant spacings (see Fig. 1)). For $d = 1$ $C(n)$ is negative and spacings are anti-correlated for any n .

C. Chaotic systems

For ballistic fully chaotic systems $K(\tau)$ has two distinct regimes⁽⁸⁾. For times $\tau \approx \tau_{min}$, with $\tau_{min} = T_{min}/h\bar{\rho}$ the rescaled period of the shortest periodic orbit, the behavior of $K(\tau)$ is non-universal, with peaks located at the periods of the shortest periodic orbits. For longer times the average behavior of $K(\tau)$ is universal and consistent with RMT. The transition between these two regimes is described semiclassically by the Hannay–Ozorio de Almeida sum rule⁽¹⁶⁾, and occurs around a cut-off time τ_* satisfying $\tau_{min} \ll \tau_* \ll 1$. Correspondingly, for energies $n \lesssim 1/\tau_*$, $\Sigma^2(n)$ agrees with the random matrix prediction, while around $n \approx 1/\tau_*$ there is a transition towards a non-universal regime, where oscillations associated to short periodic orbits around a saturation value occur. These are described⁽⁸⁾ by the non-universal term in (2.11)

$$\Sigma_{nu}^2 = \Sigma_{po}^2 + \Sigma_*^2 ,$$

with

$$\Sigma_{po}^2(n) = \frac{4}{\beta\pi^2} \sum_{r\tau_p < \tau_*} \frac{1}{r^2 |\det(M_p^r - 1)|} \sin^2(\pi nr\tau_p) \quad (2.26)$$

and

$$\Sigma_*^2 = \frac{2}{\beta\pi^2} [\text{Ci}(2\pi n\tau_*) - \log(2\pi n\tau_*) - \gamma] . \quad (2.27)$$

In Eq.(2.26) the sum is over all the classical periodic orbits p of the system, with $r = 1, 2, 3, \dots$ the number of repetitions, $\tau_p = T_p/T_H$ their normalized period and M_p the monodromy (or stability) matrix. The sum runs over orbits whose period (including repetitions) $r\tau_p$ is smaller than τ_* .

From (2.26) and (2.27) we get (cf (2.12))

$$C = C_{rm} + C_{nu} = C_{rm} + C_{po} + C_*$$

with

$$C_{po}(n) = \frac{4}{\beta\pi^2} \sum_{r\tau_p < \tau_*} \frac{\sin^2(\pi r\tau_p)}{r^2 |\det(M_p^r - 1)|} \cos(2\pi nr\tau_p) , \quad (2.28)$$

and

$$C_*(n) = \frac{1}{\beta\pi^2} \left[\text{Ci}(2\pi(n+1)\tau_*) - 2\text{Ci}(2\pi n\tau_*) + \text{Ci}(2\pi(n-1)\tau_*) - \log\left(1 - \frac{1}{n^2}\right) \right] . \quad (2.29)$$

The sum $C_{po} + C_*$ accounts for the difference between the short time dynamics of a real physical system and a pure RMT description. Indeed C_* is, with opposite sign, the RMT contribution for times $0 \leq \tau \leq \tau_*$ where a linear (diagonal) approximation of the form factor has been used. On the other hand, due to the Hannay–Ozorio de Almeida sum rule, for times $\tau \geq \tau_*$ the contribution of C_{po} coincides with $-C_*$. This means that we may extend τ_* to infinity in C_{po} and C_* , without affecting their sum. But from Eq.(2.29) we have $\lim_{\tau_* \rightarrow \infty} C_* = -(\beta\pi^2)^{-1} \log(1 - 1/n^2)$. It follows that

$$C_{\text{po}} + C_* = \frac{4}{\beta\pi^2} \sum_{p,r} \frac{\sin^2(\pi r \tau_p)}{r^2 |\det(M_p^r - 1)|} \cos(2\pi n r \tau_p) - \frac{1}{\beta\pi^2} \log\left(1 - \frac{1}{n^2}\right). \quad (2.30)$$

In contrast to Eq.(2.28), there is no restriction imposed in the latter equation and the sum extends over all periodic orbits p and their repetitions. Notice that the second term in the r.h.s. of Eq.(2.30) cancels the term C_{rm}^0 of the universal contribution C_{rm} in Eq.(2.16). The autocovariance therefore takes the form (for $n \geq 2$)

$$C(n) = \frac{4}{\beta\pi^2} \sum_{p,r} \frac{\sin^2(\pi r \tau_p)}{r^2 |\det(M_p^r - 1)|} \cos(2\pi n r \tau_p) + \frac{1}{\beta\pi^2} \left(\frac{\lambda_\beta}{n^4} + \frac{\alpha_\beta}{n^6} \right) + \mathcal{O}(1/n^8). \quad (2.31)$$

Eq.(2.31) indicates that the essential features of the autocovariances are described by the “diagonal” approximation given by the sum over the periodic orbits, which includes the universal term C_{rm}^0 given by Eq.(2.14) as well as the non-universal fluctuations due to shorter orbits². What is left out of the sum are the smooth remaining RMT terms of order $1/n^4$ and higher appearing in Eq.(2.31), which are small compared to the leading order behavior of $C_{\text{rm}}^0 \approx -(\beta\pi^2 n^2)^{-1}$ because of the size of the constants λ_β and α_β (they are of order 10^{-1}), combined to the fact that $n \geq 2$ in Eq.(2.31).

In summary, to a very good approximation the autocovariances $C(n)$ are given by the first term in Eq.(2.31)

$$C(n) = \frac{4}{\beta\pi^2} \sum_{p,r} \frac{\sin^2(\pi r \tau_p)}{r^2 |\det(M_p^r - 1)|} \cos(2\pi n r \tau_p). \quad (2.32)$$

In this sum, the long, exponentially numerous periodic orbits produce a coherent contribution given by Eq.(2.14), which is significant for low values of n and is independent of the particular position or height t of the window considered to compute $C(n)$ (i.e., is independent of T_H). On the other hand, the amplitude of the contribution of the short orbits scales like $\tau_p^2 \propto T_H^{-2}$. Therefore, in the extreme semiclassical limit $T_H \rightarrow \infty$, only the universal term contributes. However, at a finite T_H the contribution of short trajectories must be taken into account, and is particularly important for large values of n where the universal contribution is negligible. The distribution of the τ_p , their arithmetic and commensurability properties for low values of p , as well as the stability of the orbits control the form of $C(n)$ for large values of n . In the simplest (and probably general) case where only a few non-correlated short orbits significantly contribute to $C(n)$, the sum (2.32) leads to strong long range correlations between the spacings s_m . The exact form depends on the interference pattern between the orbits, with a rough estimate of the amplitude given by $4\tau_{\text{min}}^2/\beta |\det(M_{\text{min}} - 1)|$. However, coherent interference contributions between several orbits and its repetitions are of course possible, and larger fluctuations cannot be excluded.

²From a numerical point of view, instead of computing the sum in Eq.(2.31) over all the periodic orbits and its repetitions it is more convenient to truncate the sum at some $r\tau_p < \tau_*$, where τ_* is sufficiently large to ensure a RMT behavior, and add $-C_*$ (with C_* given by (2.29)) to account for the remaining part of the sum.

In order to clarify this point and to acquire further insight on the structure of $C(n)$ we rewrite the sum (2.32) in a different manner. Our purpose is to express the autocovariance in terms of classical zeta functions, a procedure that leads to a more transparent analysis. For that end, we first expand the sine function in a power series to get

$$C(n) = \frac{1}{\beta} \sum_{k=1}^{\infty} (-1)^{k+1} \frac{\pi^{2(k-1)} 2^{2k+1}}{(2k)!} \sum_{p,r} \frac{r^{2(k-1)} \tau_p^{2k}}{|\det(M_p^r - 1)|} \cos(2\pi n r \tau_p) .$$

It is convenient to split these sums in two parts $C^{(1)}$ and $C^{(2)}$ corresponding, respectively, to the two terms on the r.h.s. of the decomposition of the $2k$ -th power of the period in the numerator

$$\tau_p^{2k} = r \tau_p^{2k} - (r-1) \tau_p^{2k} . \quad (2.33)$$

The contribution of the first term to $C(n)$ may be written

$$C^{(1)}(n) = -\frac{2}{\beta\pi^2} \sum_{k=1}^{\infty} \frac{1}{(2k)!} \operatorname{Re} \frac{\partial^{2k}}{\partial n^{2k}} \sum_{p,r} \frac{e^{2\pi i n r \tau_p}}{r |\det(M_p^r - 1)|}$$

or, alternatively

$$C^{(1)}(n) = \frac{2}{\beta\pi^2} \sum_{k=1}^{\infty} \frac{1}{(2k)!} \operatorname{Re} \frac{\partial^{2k}}{\partial n^{2k}} \log \prod_{p,r} \exp \left(-\frac{e^{i r n T_p / \hbar \bar{\rho}}}{r |\det(M_p^r - 1)|} \right) . \quad (2.34)$$

The argument of the log coincides with a well known classical dynamical zeta function^{(17),(18)}

$$Z(s) = \prod_p \prod_{r=1} \exp \left(-\frac{e^{s r T_p}}{r |\det(M_p^r - 1)|} \right) , \quad (2.35)$$

and $C^{(1)}$ takes the form

$$C^{(1)}(n) = \frac{2}{\beta\pi^2} \sum_{k=1}^{\infty} \frac{1}{(2k)!} \operatorname{Re} \frac{\partial^{2k}}{\partial n^{2k}} \log Z(in/\hbar\bar{\rho}) . \quad (2.36)$$

This expression is similar, for $k=1$, to the relation found⁽¹⁹⁾ between the diagonal part of the spectral two-point correlation function and $Z(s)$ (see also the concluding remarks).

The contribution to $C(n)$ coming from the second term in the r.h.s. of Eq.(2.33), denoted $C^{(2)}$, can be obtained following similar steps to those leading to Eq.(2.36). We obtain

$$C^{(2)}(n) = -\frac{2}{\beta\pi^2} \sum_{k=1}^{\infty} \frac{1}{(2k)!} \operatorname{Re} \frac{\partial^{2k}}{\partial n^{2k}} \log F(in/\hbar\bar{\rho}) , \quad (2.37)$$

with F another dynamical zeta function

$$F(s) = \prod_p \prod_{r=2} \exp \left(-\frac{(r-1)e^{s r T_p}}{r^2 |\det(M_p^r - 1)|} \right) . \quad (2.38)$$

By this procedure, the two terms $C^{(1)}(n)$ and $C^{(2)}(n)$ are expressed without any approximation in terms of classical dynamical zeta functions. Eq.(2.32) can thus be written in the compact form

$$C(n) = \frac{2}{\beta\pi^2} \sum_{k=1}^{\infty} \frac{1}{(2k)!} \operatorname{Re} \frac{\partial^{2k}}{\partial n^{2k}} \log \left[\frac{Z(in/\hbar\bar{\rho})}{F(in/\hbar\bar{\rho})} \right]. \quad (2.39)$$

By using the fact that for chaotic systems the periodic orbits are unstable and that $r \geq 2$ in the expression of $F(s)$, it is reasonable to assume $|\det(M_p^r - 1)| \gg 1$. This leads to the approximate expression

$$F(s) \approx \prod_p \prod_{r=2} \left(1 - \frac{e^{srT_p}}{|\det(M_p^r - 1)|} \right)^{\frac{r-1}{r^2}}. \quad (2.40)$$

Equation (2.39), together with Eqs.(2.35), (2.38) or (2.40), is one of the main results of this paper. The net outcome has been a transcription of the sum over periodic orbits by an expression in terms of classical dynamical zeta functions. The first one, $Z(s)$, is well known^{(17),(18)}. Its complex zeros determine the spectrum γ_μ of the Perron-Frobenius evolution operator of a classically chaotic system. Physically, the characteristic times $(\operatorname{Re}\gamma_\mu)^{-1}$ determine the relaxation of the time evolution of classical initial clouds. The second zeta function, $F(s)$, is formally very similar to $Z(s)$ but has, to our knowledge, not been studied so far.

Assuming $Z(s)$ and $F(s)$ are entire functions that have no singularities other than poles, the beauty of Eq.(2.39) is fully revealed by considering the analytic structure of the classical zeta functions, i.e. their singular points (zeros and poles) also called *resonances*³. To simplify the discussion, consider first the zeros γ_μ of $Z(s)$ (other singular points are briefly discussed below). Factorizing $Z(s)$ in terms of the γ_μ , $Z(s) \propto \prod_\mu (s - \gamma_\mu)$, and substituting this in Eq.(2.39), it follows that the contribution to $C(n)$ of the zeros of $Z(s)$ is

$$C(n) = \frac{1}{\beta\pi^2} \sum_\mu \log \left| 1 - \frac{1}{(n + i n_\mu)^2} \right|, \quad (2.41)$$

where the n_μ are complex numbers determined by the (inverse) of the classical times measured in units of Heisenberg time

$$n_\mu = \hbar\bar{\rho} \gamma_\mu.$$

The structure of $C(n)$ as a function of the real parameter n may therefore be viewed as resulting from the contributions of classical resonances located at points n_μ in the complex plane. These are system dependent, except $\gamma_0 = n_0 = 0$ which always exists for ergodic systems and brings in the universal contribution Eq.(2.14). The remaining resonances γ_μ , $\mu \geq 1$ contribute to the non-universal oscillations of $C(n)$. Because they are located at a finite position in the complex plane (different from the origin), in the semiclassical limit $T_H \rightarrow \infty$ all the non-universal resonances are pushed towards infinity ($|n_\mu| \rightarrow \infty$ for $\mu \neq 0$), thus leaving the universal term $n_0 = 0$ as the only remaining contribution. When T_H is finite, each of the terms in (2.41) produces a peak in $C(n)$ whose shape is given by

³By an abuse of language, from now on we refer to poles *and* zeros as singular points. This terminology is justified because, up to a sign, from an analytic function point of view they both play an equivalent role in Eq.(2.39).

$$f_\mu = \frac{1}{2\beta\pi^2} \log \left[1 + \frac{2n_{\mu R}^2 - 2(n - n_{\mu I})^2 + 1}{[n_{\mu R}^2 + (n - n_{\mu I})^2]^2} \right], \quad (2.42)$$

where $n_{\mu R}$ and $n_{\mu I}$ are the real and imaginary part of n_μ , respectively. The peak is centered at $n \approx n_{\mu I}$, with a height $H = (2\beta\pi^2)^{-1} \log[1 + 2(n_{\mu R}^2 + 1)/n_{\mu R}^4]$ and width $W = 2n_{\mu R}$. Away from the maximum, f_μ has a small negative tail that tends to zero as $-[\beta\pi^2(n - n_{\mu I})^2]^{-1}$. The position of the peak is therefore controlled by the imaginary part $n_{\mu I}$, whereas the real part $n_{\mu R}$ determines its height and width.

The other singular points of $Z(s)$ and $F(s)$ contribute with similar terms as those of Eqs.(2.41) and (2.42). The only difference is a possible overall sign with respect to the zeros of $Z(s)$. Due to the structure of Eq.(2.39), the poles of $F(s)$ contribute with the same sign as the zeros of $Z(s)$, whereas the zeros of $F(s)$ and the poles of $Z(s)$ have the opposite sign. The final expression of $C(n)$ is therefore given by a superposition of the contributions of all the singular points n_{sp} of both functions, taking into account their appropriate sign,

$$C(n) = \frac{1}{\beta\pi^2} \sum_{\text{sp}} \text{sign}(\text{sp}) \log \left| 1 - \frac{1}{(n + i n_{\text{sp}})^2} \right|. \quad (2.43)$$

The larger contributions will come from resonances with the smallest real part.

III. APPLICATION TO THE RIEMANN ZEROS

We illustrate here the results of section II.C by considering the complex zeros of the Riemann zeta function $\zeta(s) = \sum_n n^{-s}$. This function is becoming an important model in the theory of quantized classically chaotic Hamiltonian systems. The connexion with a dynamical system arises when the complex zeros of $\zeta(s)$, located by the Riemann hypothesis on the line $s = 1/2 + it$, are interpreted as the eigenvalues of an hypothetical chaotic system^{(3),(20)}.

At present there are many evidences supporting the idea that asymptotically (i.e., for large t) the local statistical properties of the Riemann zeros are described by the GUE distribution of random matrices^{(21),(4)}, although more precise statements concerning the appropriate matrix ensemble have recently been made⁽²²⁾. In his extensive numerical studies of the statistical properties of the zeros, Odlyzko⁽⁴⁾ observed strong long range correlations between the spacings s_m . He also found in the Fourier transform of the autocovariances clear evidence of the contribution of small prime numbers. Here we make a quantitative comparison between his computations and the analytical results of the previous section.

For that purpose we adapt the equations of section II.C to the Riemann zeros by exploiting the analogy between a classical dynamical system and the Riemann zeta function. When comparing the Gutzwiller trace formula for the spectral density of a chaotic system on the one hand and the density of zeros on the critical line on the other (here interpreted as quantum eigenvalues), it appears that the periodic orbits of the hypothetical ‘‘Riemann dynamics’’ are labeled by the prime numbers $p = 2, 3, 5, \dots$. Many properties of these periodic orbits are known, and Table I is a list of the more relevant ones. In the same table we have also specified other quantities and correspondences, like the (leading order) behavior of the density of zeros at a height t along the critical axis.

With these definitions in hand, the autocovariance (2.32) reads

$$C(n) = \frac{2}{\pi^2} \sum_{p,r} \frac{\sin^2(\pi r \tau_p)}{r^2 p^r} \cos(2\pi n r \tau_p) . \quad (3.1)$$

The sum now runs over the prime numbers p , and $\tau_p = \log p / \log(t/2\pi)$ as indicated in Table I. The parameter t sets the height on the critical line where the correlations are computed. In Figs. 2 and 3 the theoretical prediction (3.1) is compared with numerical values (“data”) computed by Odlyzko. The agreement is good, although some small deviations remain. Important differences with respect to the RMT result are observed already at $n \approx 3$. For small values of n (Fig. 2) the typical amplitude of the non-universal fluctuations is of order 10^{-3} . For larger values of n (Fig. 3), the amplitude of the oscillations is of order 10^{-2} , confirming the existence of strong long range correlations. Indeed, assuming that the s_m are uncorrelated variables, the statistical fluctuations due to finite size effects are estimated⁽⁴⁾ to be of order 10^{-4} . Besides their amplitude, Fig. 3 shows the existence of sign correlations between several consecutive points.

It is instructive to look at the structure of $C(n)$ on larger scales (Fig. 4). $C(n)$ is computed from Eq.(3.1), which follows very closely the numerical results of Odlyzko. For relatively small separations $50 < n < 500$, $C(n)$ presents a remarkable behavior, with a dominant small positive correlation “punctuated” by large peaks of anti-correlation (made of 3 to 4 spacings). Qualitatively, the large peaks are produced by the constructive interference of a relatively small number of short periodic orbits. Indeed, we find that the qualitative features of the main resonances in Fig. 4(a) are reproduced by summing in Eq.(3.1) over approximately 12 prime numbers only (without repetitions). As n increases the isolated peaks tend to disappear, as well as the asymmetry of the plot with respect to the horizontal axis (cf part (b) and (c) of Fig. 4). As we shall now see, this peculiar structure finds a very simple explanation within the general framework based on the classical zeta functions presented in section II.C.

The first step required to write $C(n)$ as a resonance formula corresponding to Eqs.(2.39) and (2.43) is to identify the classical dynamical zeta functions associated to the “Riemann dynamics”. This is achieved by computing $Z(s)$ and $F(s)$ from Eqs.(2.35) and (2.40) using the periodic orbit correspondences of Table I (we use here for $F(s)$ the approximate equation instead of the exact one). For the former one, this procedure leads to

$$Z(s) = \prod_p (1 - p^{s-1}) = \zeta^{-1}(1 - s) , \quad (3.2)$$

where $\zeta(s) = \prod_p (1 - p^{-s})^{-1}$ is the Euler product (over the prime numbers p) representation of $\zeta(s)$. Thus, when the critical zeros of the Riemann zeta are interpreted as the eigenvalues corresponding to the quantization of some classically chaotic motion, the associated classical dynamical zeta function $Z(s)$ turns out to be the inverse of the (translated) Riemann zeta itself. Concerning the other dynamical function needed, $F(s)$, using again the periodic orbit correspondences we have

$$\prod_p \left(1 - \frac{e^{srT_p}}{|\det(M_p^r - 1)|} \right) = \prod_p (1 - p^{rs-r}) = \zeta^{-1}(r - rs) ,$$

and therefore, using the approximation (2.40) we obtain

$$F(s) = \prod_{r=2}^{\infty} [\zeta(r - rs)]^{-(r-1)/r^2} . \quad (3.3)$$

This shows the remarkable property that in the Riemann case the (approximate) dynamical function $F(s)$ is also expressed in terms of $\zeta(s)$. The dynamical zeta functions are basic tools to study the classical evolution. As we have already emphasized, the Perron-Frobenius operator controls the time evolution of classical statistical averages⁽¹⁸⁾. We have here computed two of these classical functions for the ‘‘Riemann dynamics’’ which, for completeness, have been added to Table I.

The resulting expression for the autocovariances written in terms of dynamical zeta functions follows from Eqs.(2.39), (3.2) and (3.3)

$$C(n) = -\frac{1}{\pi^2} \sum_{k=1}^{\infty} \frac{1}{(2k)!} \operatorname{Re} \frac{\partial^{2k}}{\partial n^{2k}} \log \frac{\zeta(1 - in/\bar{\rho})}{\prod_{r=2}^{\infty} [\zeta(r - inr/\bar{\rho})]^{(r-1)/r^2}} . \quad (3.4)$$

To proceed further we shall exploit the analytic structure of $Z(s)$ and $F(s)$. We simply need the following factorization formula⁽²³⁾

$$\zeta(s) = \frac{e^{(\log 2\pi - 1 - \gamma/2)s}}{2(s-1)\Gamma(1+s/2)} \prod_{\kappa} \left(1 - \frac{s}{\kappa}\right) e^{s/\kappa} , \quad (3.5)$$

which shows explicitly the presence of a pole at $s = 1$, nontrivial zeros κ lying in the critical strip $0 \leq \operatorname{Re} \kappa \leq 1$, as well as trivial zeros at the poles $s = -2m$, $m = 1, 2, \dots$ of $\Gamma(1+s/2)$. Assuming the Riemann hypothesis, namely $\kappa = 1/2 + it_{\mu}$, with t_{μ} real and coming in pairs symmetrical about the real axis, using Euler’s factorization formula for $\Gamma(1+s/2)$, and deriving term by term in the sums, Eq.(3.4) leads, together with Eq.(3.5), to a resonance-type formula

$$C(n) = \frac{1}{2\pi^2} \sum_{r=1}^{\infty} \left\{ \frac{(\delta_{r,1} + 1 - r)}{r^2} \left[\log \left| 1 - \frac{1}{(n + i n_{0r})^2} \right| - \sum_{\mu} \log \left| 1 - \frac{1}{(n + i n_{\mu r})^2} \right| - \sum_m \log \left| 1 - \frac{1}{(n + i n_{mr})^2} \right| \right] \right\} . \quad (3.6)$$

The outer sum in this equation is over the repetitions. Notice a global change of sign (reflecting the structure of Eq.(3.4)) of the $r = 1$ term with respect to the $r \geq 2$ ones. The three terms inside the square brackets (of which the last two are sums) originate from the pole, the critical zeros and the trivial zeros of $\zeta(s)$, respectively. Due to the structure of Eq.(3.4) the singular points of $\zeta(s)$ appear in $C(n)$ as resonances located at new, shifted positions in the complex plane given by

$$\begin{aligned} n_{0r} &= \bar{\rho} (1 - 1/r) \\ n_{\mu r} &= \bar{\rho} [1 - (1/2 - it_{\mu})/r] \\ n_{mr} &= \bar{\rho} [1 + 2(m+1)/r] . \end{aligned} \quad (3.7)$$

Notice also, as mentioned in section II.C, that the contribution of the pole has the opposite sign with respect to the terms associated to the zeros.

Consider first the contributions of the singular points when $r = 1$. Then the resonances are located at $n_{01} = 0$, $n_{\mu 1} = \bar{\rho}(1/2 + i t_\mu)$, and $n_{m1} = \bar{\rho}(2m + 3)$. The pole n_{01} in Eq.(3.6) gives the universal term Eq.(2.14). The nontrivial zeros $n_{\mu 1}$ are located on a rescaled and shifted “critical” line, and have all the same real part, $\text{Re } n_{\mu 1} = \bar{\rho}/2$. This explains the very interesting and peculiar structure of the autocovariances: for $r = 1$ each nontrivial zero of $\zeta(s)$ contributes to $C(n)$ with a *negative* correlation peak whose shape is given by Eq.(2.42), centered at $n = \text{Im } n_{\mu 1} = \bar{\rho} t_\mu (= 55.1, 81.9, 97.4, \dots$ for $\mu = 1, 2, 3, \dots$, with $\bar{\rho} = 3.89533$ corresponding to the window used by Odlyzko in his numerical computations). These negative peaks are clearly visible in Figs. 4 and 5. The height H and width W of the peaks is almost constant as observed in part (a) of Fig. 4 because the complex resonances are all at the same distance $\bar{\rho}/2$. From section II.C we have $H = (4\pi^2)^{-1} \log[1 + 32(\bar{\rho}^2/4 + 1)/\bar{\rho}^4] (= 0.013)$ and $W = 2n_{\mu R} = \bar{\rho}$, in good agreement with the heights and widths observed in Fig. 4 and 5. The zeros t_μ are expected to produce isolated peaks up to a value $n = n_c$ where their mean level spacing (measured in units of $\bar{\rho}(t)$) becomes comparable to the width W of the peaks. This indicates the onset of a resonance overlap regime. This condition gives $n_c \approx \log(t/2\pi) \exp(2\pi) (\approx 13100$ for the value of t used in the numerical calculations). On the other hand, the contribution of the trivial zeros is small compared either to the complex zeros or to the pole due to their greater distance with respect to the imaginary axis. The curve with squares in Fig. 5 is a plot of the $r = 1$ term of Eq.(3.6) including all the singular points, compared to $C(n)$ computed from Eq.(3.1). The presence of negative resonances at the (rescaled) position of the lowest zeros was already noticed in the two-point correlation function of the Riemann zeros in Ref.(20) (see also the concluding remarks).

Consider now the contributions of the singular points with $r \geq 2$, which are at the origin of the smaller oscillations in Fig. 5. Their displacement in the complex plane as a function of r is given by Eq.(3.7). In order to simplify the discussion, we consider explicitly the critical zeros $n_{\mu r}$, but the analysis can be extended to the other singular points. Two different effects on the location of these singular points with respect to the $r = 1$ distribution occur (see Eq.(3.7)). On the one hand, as r increases their real part increases, and $\text{Re } n_{\mu r} \rightarrow \bar{\rho}$ as $r \rightarrow \infty$. This implies that the weight of their contribution to $C(n)$ decreases with increasing r . The global factor $(1 - r)/r^2$ in Eq.(3.6) goes in the same direction. On the other hand, their location is compressed towards the real axis as r increases, since $\text{Im } n_{\mu r} = \bar{\rho} t_\mu / r$. Finally, remember that the terms with $r \geq 2$ in (3.6) have the opposite sign with respect to the $r = 1$ terms.

We can therefore summarize the contribution of the critical zeros in Eq.(3.6) as follows. Each critical zero t_μ produces a series of peaks in the autocovariance. The main one has a *negative* sign and is located at $n = \bar{\rho} t_\mu$. Decorating the main resonance there is a set of smaller *positive* peaks located at $n = \bar{\rho} t_\mu / 2, \bar{\rho} t_\mu / 3, \dots$ (with height diminishing as $H = (r - 1)(4\pi^2 r^2)^{-1} \log[1 + 2((\text{Re } n_{\mu r})^2 + 1)/(\text{Re } n_{\mu r})^4]$). Therefore, at a given value of n , the main contributions to $C(n)$ come, with decreasing importance, from zeros located at $t_\mu = n/\bar{\rho}, 2n/\bar{\rho}, 3n/\bar{\rho}, \dots$. The smaller oscillatory structure observed around a given n is thus due to zeros located $r = 2, 3, \dots$ times higher up the critical axis, thus producing an interference pattern to which a large number of nontrivial zeros are contributing with decreasing weight. The curve with diamonds in Fig. 5 is a plot of Eq.(3.6) including up to

the $r = 3$ terms. We observe that including terms higher than $r = 1$ the agreement with the result obtained from Eq.(3.1) has greatly improved, and that the most important features are reproduced. Even peaks up to the third generation are easy to identify. For example, the small positive peak located at $n \approx 18.4$ corresponds to the third-order sub-resonance of the first Riemann zero $\bar{\rho}t_1/3$, with $t_1 \approx 14.13$. The resonance formula Eq.(3.6) thus allows for a simple and transparent interpretation of the structure of $C(n)$. In contrast to the periodic orbit sum Eq.(3.1), it allows to control the amount of complexity to be included *hierarchically*.

Another interesting feature are the anomalously large peaks observed occasionally in $C(n)$, as in part (b) of Fig. 4. As mentioned before, at the height t fixed by the actual numerical computations each complex zero of $\zeta(s)$ produces a peak in $C(n)$ of height $H \approx 0.013$ up to values $n \leq n_c$. However, this is true on average, and statistical fluctuations of the spacings between consecutive zeros may produce interference effects between neighboring peaks. In some extreme cases, we may have two zeros which are very close to each other (on the scale of the width of the peaks). The occurrence of zeros whose distance is much smaller than the mean spacing is called Lehmer phenomenon, and is closely related to the Riemann hypothesis⁽⁴⁾. Whenever this unlikely phenomenon between two zeros occurs, their contributions to $C(n)$ will add coherently and produce a peak twice larger than the contribution associated to an isolated zero. To illustrate this, we display in Fig. 6 the real function

$$\mathcal{Z}(t) = \exp(i\theta(t)) \zeta(1/2 + it) , \quad (3.8)$$

with $\theta(t) = \text{Im} \log \Gamma(1/4 + it/2) - (t \log \pi)/2$. The presence of two almost degenerate zeros at $t = 7702/\bar{\rho} = 1977.24$ can be observed. This explains the large peak in $C(n)$ of size $H \approx 0.026$ observed at $n = 7702$ in part (b) of Fig. 4.

The remarkable fact that, as for the optical image produced by two mirrors face to face, the low-lying zeros of the Riemann zeta function emerge as a decaying infinite sequence of replications when looking at the correlation of zeros located at an arbitrary height t on the critical axis appears more as a conspiracy than as a generic feature of a dynamical system, although this deserves further study. The origin of this singular property seems to be associated to three (apparently unrelated) peculiarities of the Riemann zeros which conspire to produce this effect: (i) the trace formula for their density is exact, (ii) the period of the periodic orbits, $T_p = \log p$, does not depend on energy (energy corresponds here to the location t on the critical axis), and (iii) the monodromy matrix has only one expanding eigenvalue.

IV. SUMMARY AND CONCLUSIONS

In the present paper autocovariances $C(n)$ of two spacings between consecutive levels located n levels apart ($n = 1, 2, \dots$) are studied. Whereas the two-point correlation function $R_2(\epsilon)$ can be viewed as the curvature of the number variance Σ^2 , $C(n)$ represents (to within a sign) a discrete version of it. This fact implies that the effects present on the form factor (Fourier transform of R_2) on the scale of the Heisenberg time T_H are absent on $C(n)$ (or on its Fourier transform). In particular, we find that the non-analytic oscillatory structure

of the RMT result of $R_2(\epsilon)$, usually associated to off-diagonal contributions in semiclassical theories, are absent in $C(n)$ which is, in the universal regime, a monotonic function. The off-diagonal semiclassical contributions are here expected to reproduce the smooth higher-order corrections written in Eq.(2.31).

We first derive expressions for the autocovariance within the RMT of Wigner-Dyson. They are approximate but accurate. In particular, it is shown that the autocovariances in RMT are negative, monotonic functions of n , and that for large n they vanish like $-1/\beta\pi^2n^2$. The expressions found can be compared to those obtained using a similar but alternative route proposed in a previous paper. Both methods have their own advantages and drawbacks. The method adopted here allows to express systematically selected information on the form factor in terms of covariances. This is first illustrated for the case of quantum systems which are classically diffusive. An explicit expression of the autocovariances is given which consists of a universal (random matrix) contribution plus a diffusive term which depends on the dimensionality d of the system. The latter, which appears to be identically zero for two-dimensional systems, dominates the large n behavior of the autocovariances and has opposite sign for $d = 1$ and $d = 3$. Large distant spacings are negatively correlated (anti-correlated) in one dimension and positively correlated in three dimensions. Finally, for any dimension if one neglects the finest time scale given by the elastic mean free time, autocovariances tend to zero in the large n limit.

Section II.C (study of quantum systems which are classically chaotic) and section III (application to the zeros of the Riemann ζ -function) constitute the main body of the paper. By using periodic orbit theory we arrive at an accurate formula for the autocovariances $C(n)$ in terms of a diagonal approximation (Eq.(2.32)). The important time scales are the Heisenberg time (which is taken as unity) and the period of a short periodic orbit τ_{min} . Based on this result, we then find an expression of the autocovariances in terms of a sum over derivatives of the usual (classical) dynamical zeta function $Z(s)$ and another (classical) zeta function $F(s)$ closely related to it (Eq.(2.39)). The interpretation of the singular points of $Z(s)$ is well known (relaxation of an initial classical cloud, as given by the eigenvalues of the Perron-Frobenius operator). In contrast, we are not aware of a similar discussion of $F(s)$. Its study remains an open problem, in particular its analytic structure and interpretation. Presumably that as far as autocovariances (and the two-point correlation function) are concerned, $Z(s)$ gives the main behavior and the role of $F(s)$ is limited to provide some additional finer structure. At any rate, it is the location in the complex plane of the singular points (zeros and poles) of $Z(s)$ and $F(s)$ that determine the structure of $C(n)$ through a resonance-type formula (Eq.(2.43)). The location of the classical singular points are rescaled by the Heisenberg time $T_H = h\bar{\rho}$. For ergodic systems, in the semiclassical limit $T_H \rightarrow \infty$, only the zero of $Z(s)$ at the origin gives a non-negligible contribution and $C(n)$ takes the universal form (2.14). At finite T_H the non-universal singular points contribute significantly.

The expression of $C(n)$ in terms of classical zeta functions is easy to extend to the two point correlation function $R_2(\epsilon) = 1 - Y_2(\epsilon)$. Using Eq.(2.9) as starting point, and by similar steps as before we obtain, instead of Eq.(2.31), the result

$$R_2(\epsilon) - 1 = \frac{4}{\beta} \sum_{p,r} \frac{\tau_p^2}{|\det(M_p^r - 1)|} \cos(2\pi\epsilon r \tau_p) + (R_2^{RMT}(\epsilon) - 1) + \frac{1}{\beta\pi^2\epsilon^2}, \quad (4.1)$$

where we are assuming an average over a small energy window that kills some highly os-

cillatory frequencies in the sum over periodic orbits. R_2^{RMT} is the usual two-point function of RMT. As mentioned in Section II.A, the random matrix correction to the diagonal sum involves a non-analytic oscillatory behavior contained in $R_2^{RMT}(\epsilon)$ (cf Eq.(2.20)), and which is absent in $C(n)$. Due to this and contrary to the autocovariances of spacings, the diagonal approximation is a poorer approximation for R_2 . The term $(\beta\pi^2\epsilon^2)^{-1}$ plays here the role $-C_{\text{rm}}^0(n)$ is playing for the autocovariances, and compensates the smooth large- ϵ decaying behavior of $R_2^{RMT}(\epsilon)$. The other important difference between (4.1) and Eq.(2.31) is the presence of the square of the sine function in the latter, which is due to the discrete nature of the curvature $C(n)$.

Exactly as for the autocovariances we may express the diagonal sum in Eq.(4.1) in terms of classical dynamical zeta functions

$$R_2^{diag}(\epsilon) - 1 = \frac{1}{\beta\pi^2} \text{Re} \frac{\partial^2}{\partial \epsilon^2} \log \left[\frac{Z(i\epsilon/\hbar\bar{\rho})}{F(i\epsilon/\hbar\bar{\rho})} \right]. \quad (4.2)$$

The relation connecting the diagonal part of R_2 and $Z(s)$ was found in Ref.(19) (where an extension to include the non-diagonal part was also given, see also Ref.(24)). Here we have generalized this by including a second dynamical zeta function, which we have explicitly computed in the case of the Riemann ζ -function and turns out to bring non-negligible contributions. Its contribution was usually expressed as a sum over periodic orbits, and not written in terms of the more transparent approach used here. In contrast to Eq.(4.2), the existing relation between $C(n)$ and the dynamical zeta functions Eq.(2.39) involves a sum over derivatives, whose first term coincides with Eq.(4.2). The summation leads to different shapes of the resonances of $C(n)$ compared to those of Eq.(4.2).

These two quantities – the spacings autocovariance $C(n)$ and the spectral two-point correlation $R_2(\epsilon)$ – illustrate the manifestation of classical resonances in quantum correlations. This connexion seems however to be more general, as shown by a recent experiment⁽²⁵⁾ on microwave scattering in an open system.

We finally study, in the framework developed in the previous section on chaotic systems, the autocovariances $C(n)$ for the case of zeros on the critical line of the Riemann ζ -function (section III). This is achieved by using the well known “dictionary” which translates quantum (eigenvalues of the Hamiltonian or evolution operator) and classical (periodic orbits, actions,...) information into the corresponding ζ -function quantities, namely imaginary part of zeros (“quantum”) and prime numbers (“classical”) (cf Table I).

We first derive a periodic orbit sum (over primes and its repetitions) expression of the autocovariances $C(n)$. After a short universal random matrix regime, $C(n)$ is dominated with increasing n by the non-universal terms, encoded here in the prime numbers. We check the accuracy of the formula obtained by comparing to partial existing “data” of Odlyzko. The agreement is good. It is unclear whether the remaining differences are due to the approximations made in our derivation or to numerical inaccuracies. Probably to both. This deserves further study.

Better insight can be gained by writing the autocovariances in terms of the (classical) dynamical zeta functions $Z(s)$ and $F(s)$. Extending the existing “dictionary” which connects dynamical properties and ζ -function properties, one finds that the classical dynamical zeta functions $Z(s)$ and $F(s)$ are expressed in terms of the Riemann ζ -function itself (Eqs.(3.2) and (3.3), and Table I). This remarkable connection between classical operators and the

function that determines the “quantum spectrum” leads to a resurgence phenomenon of the low lying Riemann zeros in the autocovariances computed at a height $t \gg 1$ on the critical line. This phenomenon is clearly displayed in a resonance formula obtained for $C(n)$ (Eq.(3.6)) which is particularly appealing and which allows to interpret most of the features observed from data as predicted by the periodic orbit expression.

The salient qualitative and quantitative features of the autocovariances $C(n)$, mentioned in what follows, are easy to read off from the resonance formula. They have been checked by comparing to the results obtained from the periodic orbit summation formula, which is accurate but comparatively opaque. At a given height t on the critical line, which sets the scale $\bar{\rho}$, $C(n)$ starts as the random matrix prediction. Up to a critical value n_c ($\propto \log t$) of n , the low lying zeros of ζ produce (negative) well isolated constant-amplitude peaks centered at $\bar{\rho}t_\mu$, where t_μ is the imaginary part of the μ -th Riemann zero. One therefore neatly sees the *low-lying zeros* of ζ appearing in the autocovariances computed at an arbitrary height on the critical line. The effect of the other dynamical zeta function, $F(s)$, is to provide further structure, namely smaller (positive) peaks at values $\bar{\rho}t_\mu/2, \bar{\rho}t_\mu/3, \dots$, with decreasing importance. One therefore sees the low-lying zeros lurking as sub-resonant (positive) peaks. Beyond n_c , the overlapping resonance regime sets in, and $C(n)$ oscillates erratically. Occasionally, when two zeros of ζ are very close (Lehmer phenomenon) at a height t , they give rise to a peak with double amplitude at $n = \bar{\rho}t$.

Let us finally conclude by noticing that in several respects it is easier to apply the formalism developed in Section II to the Riemann case, as we have done here, than to a real dynamical system. It may be worth to study in some detail some of the best known maps, like the cat or the baker map, from the present viewpoint. The physical significance of the dynamical zeta function $F(s)$ introduced here may then become clearer.

Acknowledgments: We are grateful to A. Odlyzko for discussions and to the ECOS-Sud Franco-Argentinian scientific cooperation program (A98E03) for partial financial support.

REFERENCES

1. M. C. Gutzwiller, *Chaos in Classical and Quantum Mechanics* (Springer Verlag, New York, 1990).
2. O. Bohigas, P. Leboeuf and M. J. Sánchez. *Physica D* **131**, 186 (1999).
3. M. V. Berry, in *Quantum Chaos and Statistical Nuclear Physics* edited by T. H. Seligman and H. Nishioka, *Lectures Notes in Physics* **263**, (Springer Verlag, Berlin, 1986) p.1.
4. A. M. Odlyzko, *Math. Comp.* **48**, 273 (1987); “The 10^{20} -th zero of the Riemann zeta function and 70 million of its neighbors”, AT & T Report, 1989 (unpublished); “The 10^{20} -th zero of the Riemann zeta function and 175 million of its neighbors”, AT & T Report, 1992 (unpublished).
5. O. Bohigas and M.-J. Giannoni, in *Lecture Notes in Physics* **209**, (Springer, Berlin, 1984) p.1.
6. P. Leboeuf and M. Sieber, *Phys. Rev. E* **60**, 3969 (1999).
7. J. B. French, P. A. Mello and A. Pandey, *Ann. Phys.* **113**, 277 (1978). T. A. Brody, J. Flores, J. B. French, P. A. Mello, A. Pandey and S. S. M. Wong, *Rev. Mod. Phys.* **53**, 385 (1981); J. B. French, V. K. B. Kota, A. Pandey and S. Tomsovic, *Ann. Phys.* **181**, 198 (1988); A. Pandey, unpublished (1982).
8. M. V. Berry, *Nonlinearity* **1**, 399 (1988).
9. G. Montambaux in *Quantum Fluctuations* edited by S. Reynaud, E. Giacobino and J. Zinn-Justin, *Les Houches Session LXIII*, (North Holland, Amsterdam, 1997) p.387.
10. M. L. Mehta, *Random Matrices* (Academic Press, New York, 1991), 2nd ed.
11. M. L. Mehta and F. J. Dyson, *J. Math. Phys.* **4**, 713 (1963).
12. A. Pandey, in Ref.(3), p.98.
13. A. Altland and Y. Gefen, *Phys. Rev. Lett.* **71**, 3339 (1993).
14. B. L. Altshuler and B. I. Shklovskii, *Zh. Eksp. Teor. Fiz.* **91**, 220 (1986) [*Sov. Phys. JETP* **64**, 127 (1986)].
15. K. Efetov, *Adv. Phys.* **32**, 53 (1983).
16. J. Hannay and A. M. Ozorio de Almeida, *J. Phys. A* **17**, 3429 (1984).
17. P. Cvitanović and B. Eckhardt, *J. Phys. A* **24**, L237 (1991).
18. D. Ruelle, *Statistical Mechanics, Thermodynamic Formalism* (Addison-Wesley, Reading, MA, 1978); P. Gaspard, *Chaos, Scattering and Statistical Mechanics* (Cambridge University Press, Cambridge UK, 1998).
19. O. Agam, B. L. Altshuler and A. Andreev, *Phys. Rev. Lett.* **75**, 4389 (1995).
20. M. V. Berry and J. Keating, *SIAM Review* **41**, 236 (1999).

21. H. L. Montgomery, *Proc. Symp. Pure Math.* **24**, 181 (1973); D. A. Goldston and H. L. Montgomery, *Proc. Conf. at Oklahoma State Univ.*, edited by A. C. Adolphson *et al*, 183 (1984).
22. N. M. Katz and P. Sarnak, *Bull. Amer. Math. Soc.* **36**, 1 (1999).
23. E. C. Titchmarsh, *The Theory of the Riemann Zeta Function* (Clarendon Press, Oxford, 1986), 2nd edition.
24. E. Bogomolny and J. Keating, *Phys. Rev. Lett.* **77**, 1472 (1996).
25. K. Pance, W. Lu and S. Sridhar, *Phys. Rev. Lett.* **85**, 2737 (2000).

TABLES

| | Correspondences |
|--|--|
| label of periodic orbits | prime numbers p |
| Planck constant | $\hbar \rightarrow 1$ |
| symmetry class | $\beta \rightarrow 2$ |
| asymptotic limit | $t \rightarrow \infty$ |
| (asymptotic) density | $\bar{\rho} \rightarrow \log(t/2\pi)/(2\pi)$ |
| Heisenberg time | $T_H = h\bar{\rho} \rightarrow \log(t/2\pi)$ |
| action | $S_p \rightarrow t \log p$ |
| period | $T_p \rightarrow \log p$ |
| rescaled period | $\tau_p \rightarrow \log p / \log(t/2\pi)$ |
| Lyapounov exponent | $\lambda_p \rightarrow 1$ |
| stability factor | $ \det(M_p^r - 1) \rightarrow p^r$ |
| dynamical zeta functions | $Z(s) \rightarrow \zeta^{-1}(1-s)$ $F(s) \rightarrow \prod_{r=2}^{\infty} [\zeta(r-s)]^{(r-1)/r^2}$ |
| “ergodic” zero of $Z(s)$ | $\gamma_0 \rightarrow$ pole of $\zeta(s)$ |
| other zeros and poles of $Z(s)$ and $F(s)$ | \rightarrow zeros of $\zeta(s)$ |

TABLE I. Correspondences for the “Riemann dynamics”. The last three entries are discussed in the text.

FIGURES

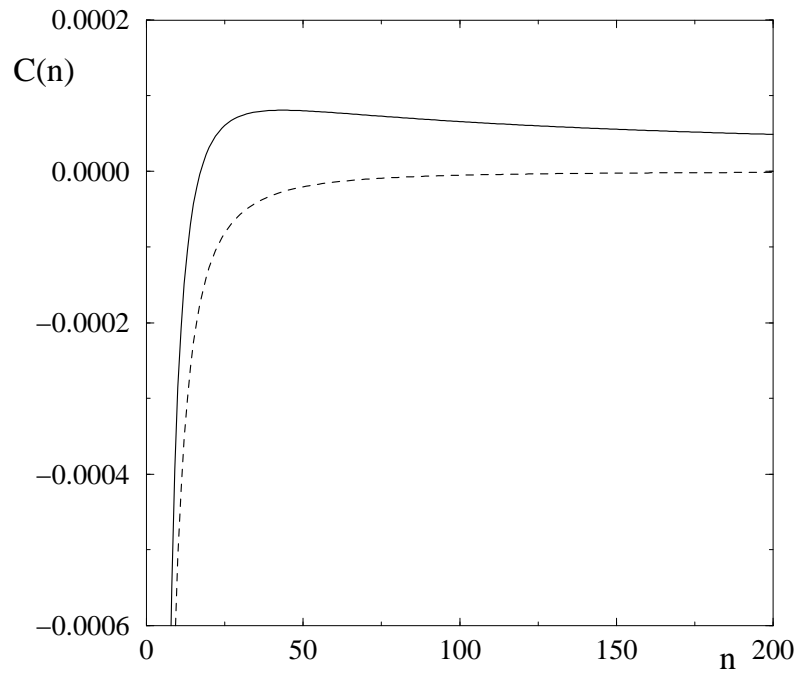


FIG. 1. Spacing autocovariances for a three-dimensional diffusive system, with $\beta = 2$. The dashed curve is the random matrix term C_{rm} ; the continuous curve includes the contribution C_{dif} , Eq.(2.25).

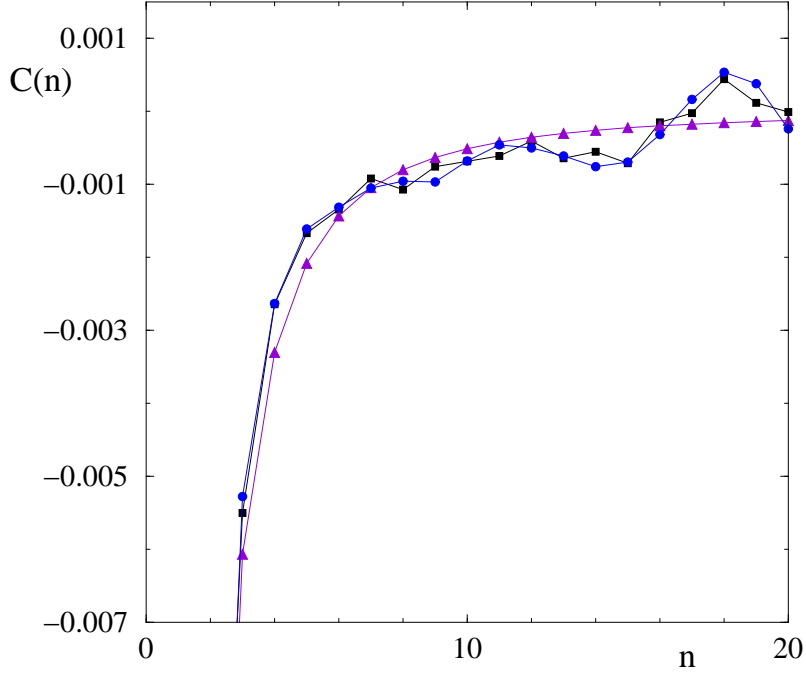


FIG. 2. Spacing autocovariances $C(n)$ in the range $n \leq 20$. Triangles: random matrix result, from Eq.(2.16). Squares: data from Odlyzko computed from Riemann zeros in an interval starting around the 10^{12} -th zero at $t = 267653395648.8475$ and containing 50000 zeros. Circles: theoretical curve, from Eq.(3.1). Points are joined by solid lines to guide the eye.

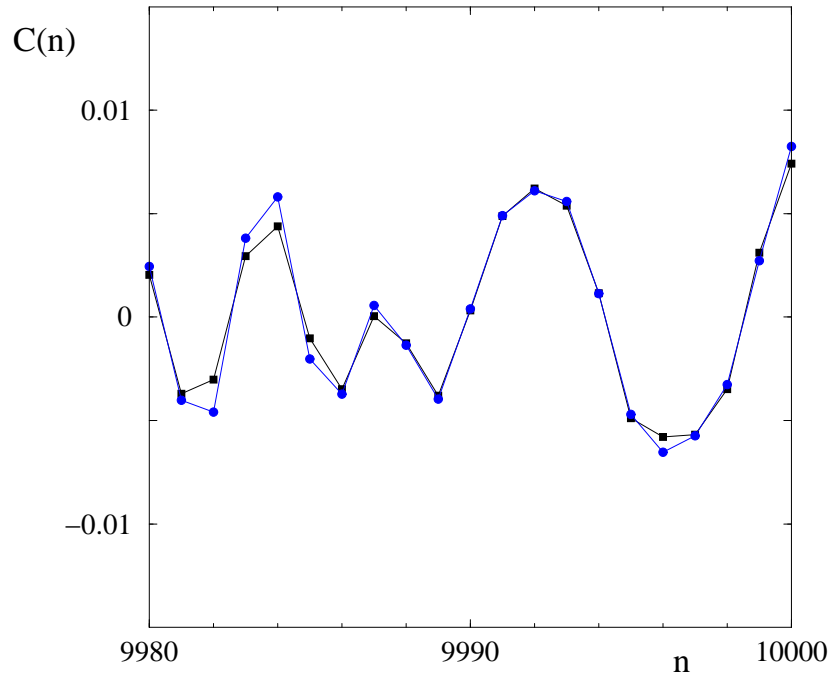


FIG. 3. Spacing autocovariances $C(n)$ for Riemann zeros in the range $9980 \leq n \leq 10000$. Squares, from data; circles, from theory, as explained in the caption of Fig. 2.

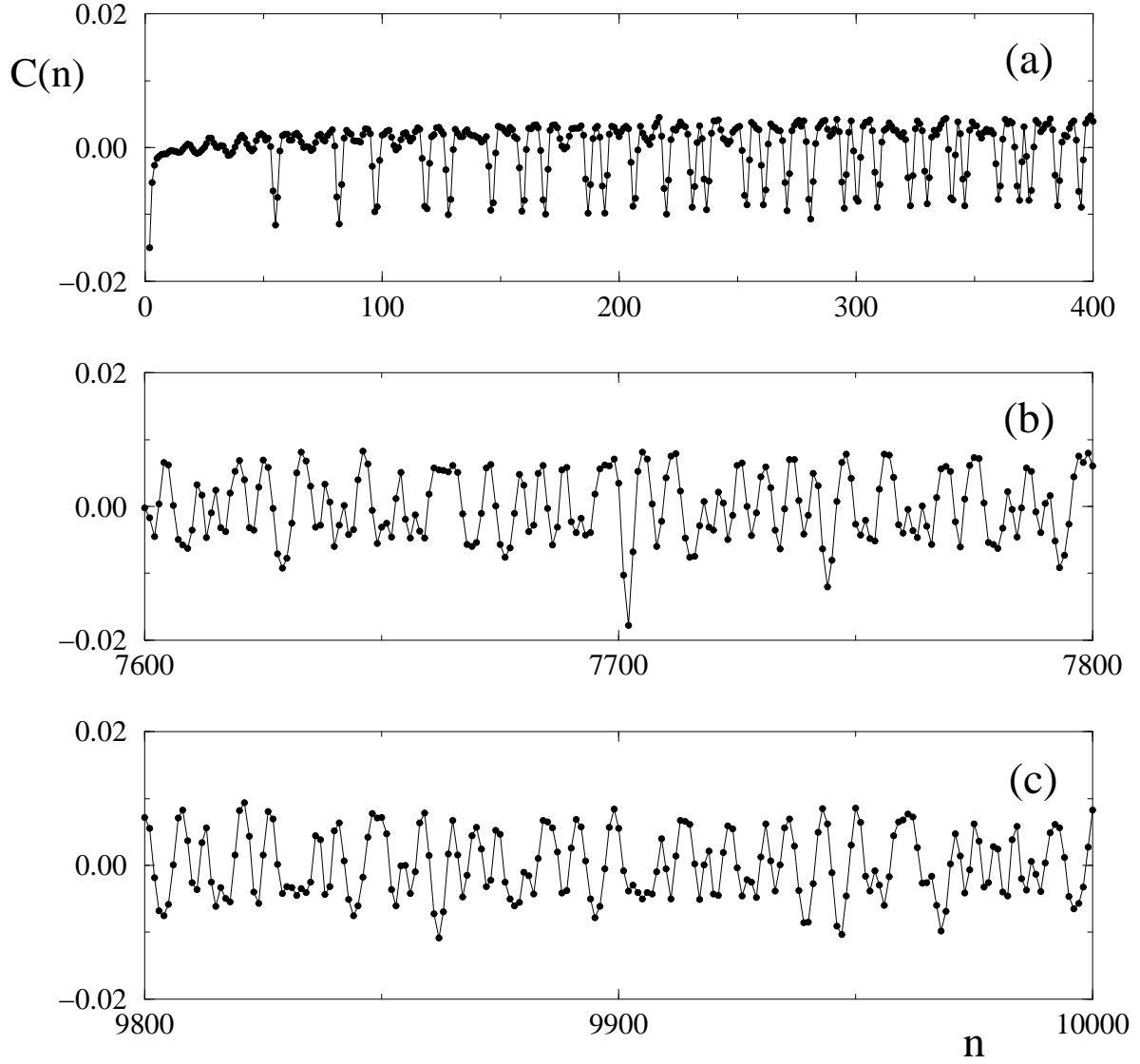


FIG. 4. Spacing autocovariances $C(n)$ for Riemann zeros for three different ranges of n to illustrate several regimes and phenomena. Circles, from theory (Eq.(3.1), see caption of Fig. 2). The last part of Fig. 4(c) corresponds to Fig. 3.

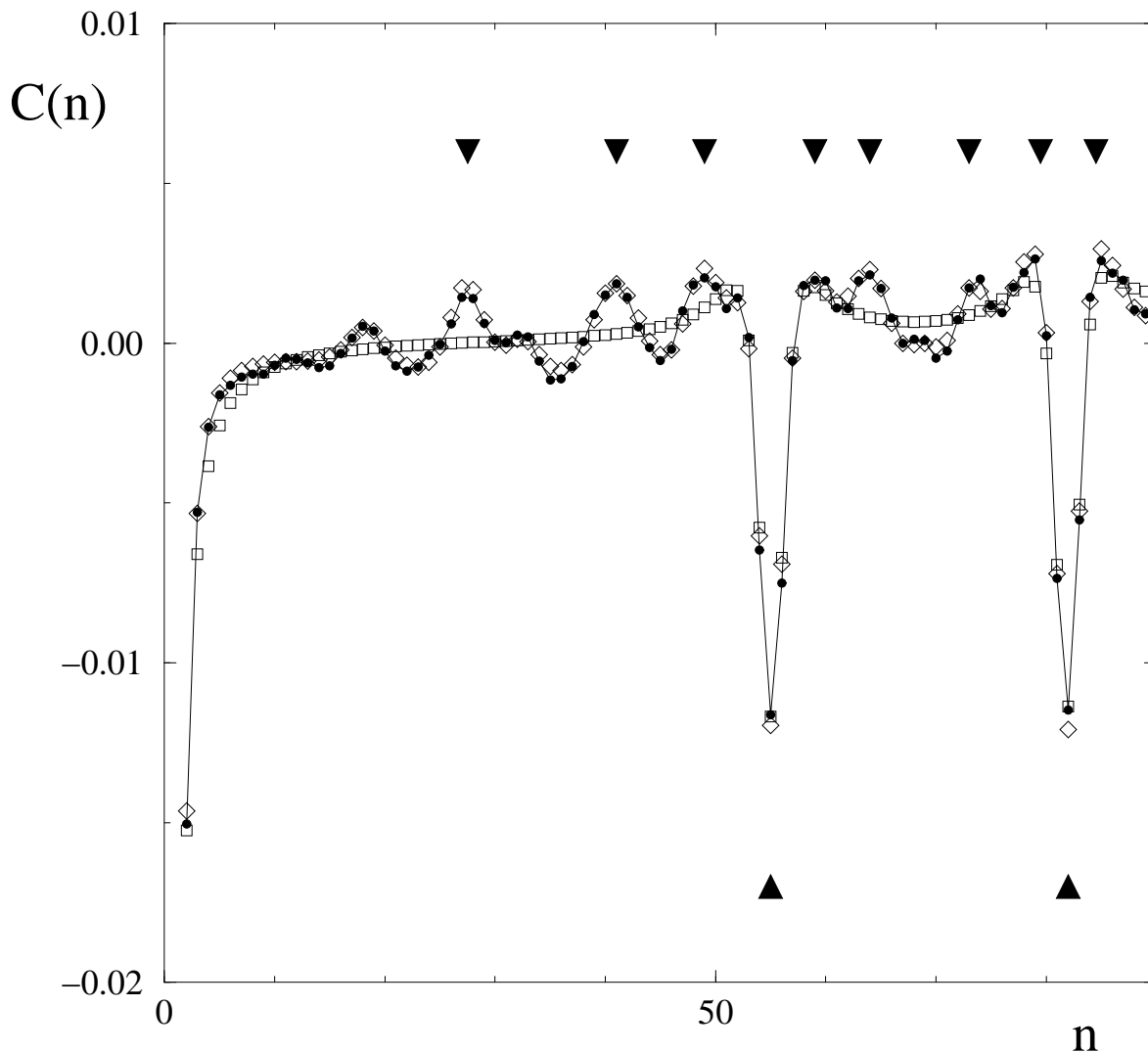


FIG. 5. Spacing autocovariances $C(n)$ for the Riemann zeros. Enlarged view of the left part of Fig. 4(a). Circles: from periodic orbit theory, as in Figs 2, 3 and 4. Squares: from the resonance formula Eq.(3.6) where only the $r = 1$ term has been kept. Diamonds: from Eq.(3.6), including up to the $r = 3$ term. The two arrows in the lower part of the figure indicate the rescaled position $\bar{\rho}t_\mu$ of the first two complex zeros $1/2 + it_\mu$ of $\zeta(s)$. The eight in the upper part correspond to the first sub-resonances $\bar{\rho}t_\mu/2$ of the first eight zeros of $\zeta(s)$. Some other (positive) peaks visible on the figure correspond to higher order sub-resonances.

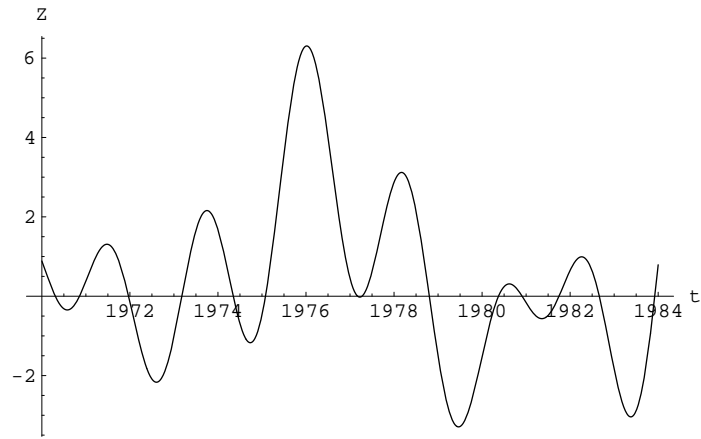


FIG. 6. The function $\mathcal{Z}(t)$, Eq.(3.8), showing two close-lying zeros of $\zeta(1/2 + it)$ around $t = 1977.2$. This almost degeneracy is at the origin of the large peak observed in $C(n)$ at $n = \bar{\rho}t = 7702$ in Fig.4(b).